Thermal lens measurements in Yb-doped YAG, LuAG, Lu$_2$O$_3$, Sc$_2$O$_3$ ceramic lasers

A Pirri[1], G Toci[2, *], M. Ciofini[3], A. Lapucci[3], L. A. Gizzi[4], L. Labate[4], L. Esposito[5], J. Hostaša[5] and M. Vannini[2]

[1]Istituto di Fisica Applicata "N. Carrara", IFAC-CNR, Via Madonna del Piano 10 C, 50019 Sesto Fiorentino (FI), Italy.

[2]Istituto Nazionale di Ottica, INO-CNR, Via Madonna del Piano 10 C, 50019 Sesto Fiorentino (FI), Italy.

[3]Istituto Nazionale di Ottica, INO-CNR, Largo Enrico Fermi 6, 50125 Firenze, Italy.

[4]Istituto Nazionale di Ottica, INO-CNR, Via G. Moruzzi 1, 56124 Pisa, Italy.

[5]Istituto di Scienze e Tecnologie delle Ceramiche, ISTEC-CNR, Via Granarolo 64, 48018 Faenza, Italy.

E-mail: guido.toci@ino.it

Abstract: we report the last experimental results obtained measuring the thermal lens effect in Yb(1$at.$%):Lu$_2$O$_3$, Yb(1$at.$%):Sc$_3$O$_3$, Yb(10$at.$%):LuAG and Yb(10$at.$%):YAG ceramics. The experimental set-up apparatus using a Shack-Hartmann wavefront sensor allows the comparison of the thermal lens obtained under lasing and non lasing conditions, in order to highlight differences in the thermal loading.

1. Introduction

Diode pumped solid state lasers based on Yb-doped YAG [1-2] and LuAG ceramic [3-4] have shown some of the most promising results in the last few years, ranging from CW powers in the kW range to Kerr-lens mode-locked operation with fs pulses [2, 5-7].The use of materials having an appropriate thermal behaviour is extremely important because it can significantly improve the laser performance avoiding the possible decrease of the output power and the deterioration of the beam quality. The ceramic technology is playing a special role enabling the production of two important sesquioxides such as Lu$_2$O$_3$ [8-11] and Sc$_2$O$_3$ [12-14]. Basically, the thermal conductivity decreases with the doping level due to the different atomic weight of Yb^{3+} and the substituted host cation. LuAG and Lu$_2$O$_3$ play a special role because of their initial high thermal conductivity (8.0 W/mK [15] and 12.2 W/mK respectively [16]) is found to be insensitive to doping. Among the effects determining the thermo-mechanical behaviour such as the thermal lens, the re-absorption as well as the thermal conductibility,

---

*   To whom any correspondence should be addressed

the former is the most difficult to manage because it can dramatically change the resonator stability conditions and the diffraction losses.

In this work, we report the last experimental results obtained measuring the thermal lens effect in Yb-doped YAG, LuAG, Lu_2O_3, Sc_2O_3 ceramics. It was done by using an experimental set-up apparatus based on a Shack-Hartmann wavefront sensor, which allows the comparison of the thermal lens obtained in lasing and non lasing conditions in order to point out the differences in the thermal load.

2 Experimental apparatus

The experimental apparatus was designed to allow the measurement of the thermal lens in lasing and nonlasing samples, under longitudinal pumping. For this purpose the samples are inserted in a longitudinally pumped laser cavity, and a probe beam is used to measure the thermal lens effect. The pump source is a semiconductor laser emitting at 936 nm. The output of the laser is coupled in an optical fiber (200 μm diameter, 0.22 NA) whose output is refocused and magnified by a pair of achromatic doublet on a waist with 500 μm diameter $@1/e^2$ located in the center of the sample. A maximum incident pump power of 21.8 W CW was used in the experiments.
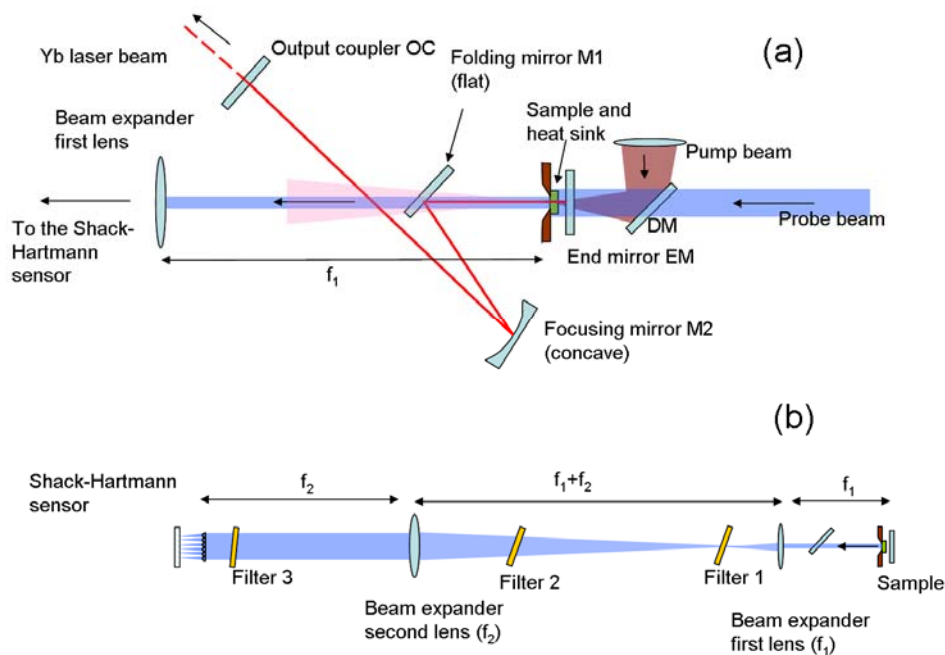
Figure 1: Experimental set-up for the measurement of the wavefront thermal distortion and of the thermal lens dioptric power. (a): Pump source: HeNe laser; Pump laser: CW fibre-coupled diode laser at 936 nm; DM: dichroic mirror; EM: End cavity mirror; M1: flat mirror; M2:spherical mirror (focal length 100 mm); OC: output coupler mirror. (b): Schematics of the probe beam path between the sample and the sensor.

The pump beam is injected into the laser cavity by the dichroic mirror DM and then through the end mirror EM (dichroic, high transmission at the pump wavelength, high reflection at the laser wavelength). The cavity is folded with the flat mirror M1 and with the spherical mirror M2 (focal length 100 mm), and it is closed by the output coupler OC. The overall distance between M2 and EM is 113 mm, and the distance between M2 and OC is 210 mm. The fundamental cavity mode radius on the waist located at the mirror EM was calculated as 100 μm for the "cold" cavity. The samples are

brazed with Indium on a copper heat sink with a central circular aperture having a diameter of 2.5 mm, on the opposite side with respect to the incidence of the pump beam.

The thermal lens is probed by a beam emitted by a HeNe laser, see Fig. 1. The beam is expanded and collimated, sent into the sample collinearly with the pump beam through the mirrors DM and EM, and extracted from the cavity through the mirror M1. The probe beam illuminates the whole clear aperture of the sample holder. The wavefront distortion induced by thermal effects is measured by means of a Shack-Hartmann wavefront sensor (ML4010 by Metrolux GmbH, area 8.98 x 6.71 mm^2 and 200 μm pitch of the microlenses array). In order to measure the wavefront distortion occurring over an area of about 500 μm diameter, the probe beam was expanded by an afocal telescope formed by the two positive lenses with nominal focal lengths $f1$=155 mm and $f2$=750 mm placed at a distance $d=f1+f2$.

The sample and the sensor are placed in the conjugate planes of the telescope. The probe beam at the output of the sample is then reimaged on the sensor with a magnification $M=f2/f1$, without any further wavefront curvature introduced by the telescope. The magnification of the telescope was accurately measured and it resulted M=4.81. Several filters are used to reject the residual pump beam that would otherwise impinge on the sensor. The thermal deformation of the wavefront is measured at several levels of incident pump power. A circular portion of the wavefront with radius a corresponding to the pumped area of the sample is then selected and analyzed by fitting with Zernike polynomials up to the 6th order. The effective dioptric power D_{th} of the thermal lens is then calculated with the formula:

$$D_{th} = \frac{1}{f_{th}} = \frac{a^2}{4 Z_{2,0}} M^2$$

(1)

where $Z_{2,0}$ is the coefficient of the Zernike polynomial with radial index 2 and azimuthal index 0, corresponding to the wavefront defocus. In this analysis, we adopted a value of a=1.2 mm (on the sensor plane), corresponding to the pump beam radius at $1/e^2$ (*i.e.* 250 μm) on the sample plane. Due to the different absorption featured by the crystals, the dioptric power of the thermal lens was analyzed as a function of the absorbed pump power.

3. Experimental results and comments

Figures 2 (a) and (b) report the thermal lens results obtained with the Yb(10*at.* %):YAG and Yb(10*at.* %):LuAG respectively. Figures 3 (a) and 3 (b) show the measurements obtained with the Yb(1*at.* %):Sc$_2$O$_3$ and Yb(1*at.* %):Lu$_2$O$_3$ respectively. The lasing condition was obtained by an OC with a low transmission of T=2% in order to maximize the intracavity circulating power and, in turn, the difference in thermal load between lasing and non-lasing conditions. In non lasing conditions the dioptric power D of the thermal lens is expected to scale linearly with the absorbed pump power P_{abs}, according to the following relation [18]:

$$D_{off} = \Delta_{off} P_{abs} = A_{off}\left(1 - \eta_r \frac{\lambda_P}{\lambda_F}\right) P_{abs}$$

(2)

where P_{abs} is the absorbed pump power. The quantity in brackets express the fraction of the absorbed pump power that is converted in heat and it is influenced by the radiative quantum efficiency η_r; λ_P and λ_F are the pump wavelength and the average fluorescence wavelength respectively. The constant A_{off} incorporates the thermo-optical and the thermal properties of the material, as well as the geometric conditions [18].

In lasing conditions the overall probability of nonradiative decays is reduced by the stimulated emission probability that becomes dominant when the laser is pumped well above the threshold. In this latter condition the expression for the thermal lens can be modified as it follows:

$$D_{on} = \Delta_{on} P_{abs} = A_{on}\left(1 - \frac{\lambda_P}{\lambda_L}\right) P_{abs}$$

(3)

where λ_L is the lasing wavelength. It must be noticed that for the materials here considered is usually $\lambda_L > \lambda_F$; therefore, when the radiative quantum efficiency $\eta_r = 1$ the thermal load is higher under lasing than under non lasing conditions.

The value of the constant A_{on} is not necessarily the same as A_{off}, because the heat sources distribution in lasing conditions can be different from nonlasing conditions. Nevertheless if the laser is well above threshold we can make the approximation that the whole pumped region is lasing, so that the heat sources distribution becomes the same in the two cases and $A_{on} = A_{off}$.
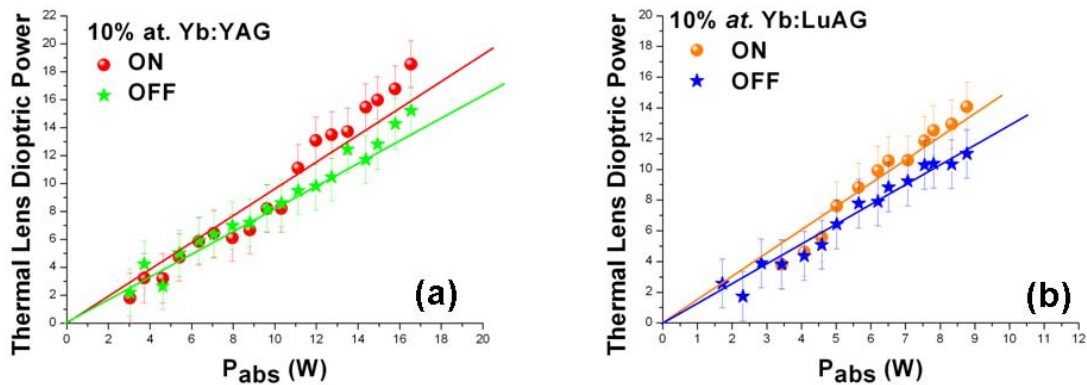
Figure 2. Thermal lens dioptric power (m^{-1}) in YAG (a) and in LuAG (b) as a function of the absorbed pump power. The solid curves are the best linear fits. ON and OFF stand for laser action on or off.

The thermal lens in the YAG and LuAG samples shows the expected linear dependence from the absorbed pump power, see Fig. 2 (a) and 2 (b); the slope in lasing and nonlasing conditions is slightly different for the reasons exposed above.
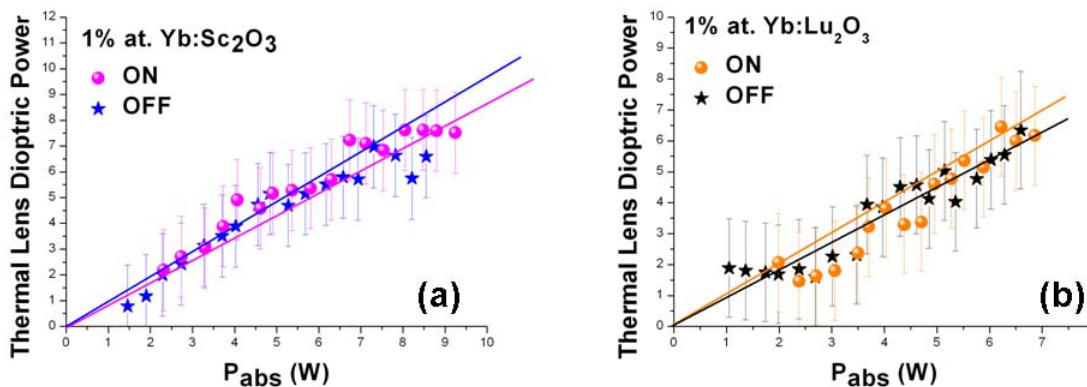
Figure 3. Thermal lens dioptric power (m^{-1}) in Sc$_2$O$_3$ (a) and in Lu$_2$O$_3$ (b) as a function of the absorbed pump power. The solid curves are the best linear fits. ON and OFF stand for laser action on or off.

From the analysis of the measurements shown in Figure 2 it appears that Yb:LuAG has a slightly smaller thermal lens effect than Yb:YAG: indeed, the slope of the thermal lens dioptic power with respect to the absorbed pump power is 0.77 (m W)$^{-1}$ for LuAG and 0.82 (m W)$^{-1}$ for YAG. In both cases the slope of the thermal lens dioptric in laser on conditions is higher than in the case of laser off. This indicates that the quantum efficiency of these two material is very close to unity (see Eq. 2).

Regarding the sesquioxides Yb:Sc_2O_3 and Yb:Lu_2O_3 (Figures 3(a) and 3(b)) the slopes of the thermal lens with respect to the absorbed pump power are respectively 1.0 and 1.1 (m W)$^{-1}$ (in laser off conditions), so Lu_2O_3 has an overall thermal lens effect slightly larger than Sc_2O_3. Moreover, the slopes in the laser on and laser off conditions are very similar, indicating that the quantum efficiency is slightly lower than in the case of the LuAG and YAG.

4. Conclusions

In conclusion, we have measured the thermal lens in several promising laser hosts doped with Yb, that is ceramic YAG, LuAG, and ceramic sesquioxides Sc_2O_3 and Lu_2O_3.

These measurements, carried out in uniform experimental conditions, allow to make a direct comparison among the different materials, showing that LuAG has a small advantage in terms of thermal lens. Moreover, the behavior of the thermal lens in laser on and laser off conditions can be analyzed in order to determine the quantum efficiency of the materials. This analysis will be the subject of forthcoming papers [18].

References

[1] Takaichi K, Yagi H, Lu J, Shirakawa A, Ueda K, Yanagitani T, Kaminskii A A 2003 Phys. Stat. Sol. A **200** R5
[2] Ikesue A, Kinoshita T, Kamata K, Yoshida K, 1995 J. Am. Ceram. Soc. **78**, 1033
[3] Pirri A, Vannini M, Babin V, Nikl M, Toci G, 2013 Laser Phys. **23** 095002
[4] Luo D, Zhang J, Xu C, Yang H, Lin H, Zhu H, Tang D, 2012 Opt. Mat. Express **2** 1425
[5] Dong J, Ueda K, Shirakawa A, Yagi H, Yanagitani T, Kaminskii A A, 2007 Opt. Express **15** 14516
[6] Yoshioka H, Nakamura S, Ogawa T, Wada S, Yoshioka H, 2009 Opt. Express **17** 8919
[7] Griebner U, Petrov V, Petermann K, Peters V, 2004 Opt. Express **12** 3125
[8] Lu J, Takaichi K, Uematsu T, Shirakawa A, Musha M, Ueda K, Yagi H, Yanagitani T, Kaminskii A A, 2002 Appl. Phys. Lett. **81** 4324
[9] Tokurakawa M, Takaichi K, Shirakawa A, Ueda K, Yagi H, Hosokawa S, Yanagitani T, Kaminskii A A, 2006 Opt. Express **14** 12832
[10] Kaminskii A A, Bagayev S N, Ueda K, Takaichi K, Shirakawa A, Ivanov S N, Khazanov E N, Taranov A V, Yagi H, Yanagitani T, 2006 Laser Phys. Lett. **3** 375
[11] Kaminskii A A, Akchurin M Sh, Becker P, Ueda K, Bohatý L, Shirakawa A, Tokurakawa M, Takaichi K, Yagi H, Dong J, Yanagitani T, 2008 Laser Phys. Lett. **5** 300
[12] Sanghera J, Frantz J, Kim W, Villalobos G, Baker C, Shaw B, Sadowski B, Hunt M, Miklos F, Lutz A, Aggarwal I, 2011 Opt. Lett. **36** 576
[13] Pirri A, Toci G, Vannini M, 2011 Opt. Lett. 36 4284
[14] Lupei V, Lupei A, Ikesue A, 2005 Appl. Phys. Lett. **86** 111118
[15] Nakao H, Shirakawa A, Ueda K I, Yagi H, Yanagitani T, 2012 Opt. Express **20** 15385
[16] Petermann K, Fornasiero L, Mix E, Peters, V, 2002 Opt. Mat. **19** 67
[17] Chénais S, Balembois F, Druon F, Lucas-Leclin G, Georges P, 2004 IEEE J. Quantum Electron. **40** 1217
[18] Pirri A, Toci G, Nikl M, Babin V, Vannini M, 2013 Opt. Express, submitted Nov. 12, 2013